The Influence of Surface Defects on the Heterogeneous Nucleation and Growth of Thin Films

J. Cardoso and M. Harsdorff

Institut für Angewandte Physik der Universität Hamburg

Z. Naturforsch. **33a**, 442–446 (1978); received February 7, 1978

In the present paper the nucleation and growth of gold on mica is investigated. By means of an image analysing computer it was possible to evaluate many electron micrographs with regard to nucleation rate, growth of crystallites and fractional part of the surface covered by crystallites. The comparison of the experimental results with nucleation theories shows that an explanation is possible by use of a simple atomic model, even in the case of substrates with defect sites.

Introduction

Point defects on surfaces should have an important influence on the statistical nucleation of metals on substrates because of the changed adsorption energy in the vicinity of the defects.

In the present paper, the nucleation and growth of gold on mica was studied in detail. Mica was an adequate substrate because of its cleavability and the generation of point defects simply by heating the substrate up to temperatures of 550 centigrade. At this temperature potassium is evaporated from the specimen, clearly visible in a quadrupol mass filter, used in the UHV-apparatus, either for monitoring the residual gas composition or to regulate the vapour beam density [1].

Gold was used because of its stability against chemical reactions.

2. Specimen Preparation

The gold was evaporated from a molybdenum crucible, heated by electron bombardement and shielded by a watercooled cylinder. The vapour beam was monitored by a quadrupol mass spectrometer and regulated with an accuracy of about 2% for many hours. The substrate surfaces were obtained by cleavage of mica sheets in the Ultra high vacuum. The prepared surfaces were then baked at a temperature of 550 °C for several hours. In the baking procedure all contaminants being present in the mica before cleavage are evaporated [2] and the desired point defect density is obtained by evaporation of potassium. After this the temperature was decreased to the required value and regulated with an accuracy of ± 1 °C.

The surface was then exposed to the incident gold vapour beam for a well defined time intervall. After the gold deposition a stabilizing carbonfilm of about 200 Å thickness was deposited on the top of the gold islands. After this another experiment was performed by use of another cleavage plane, usually under the same experimental conditions as to substrate temperature and deposition rate but with a different deposition time. Using a substrate holder with six simultaneously cleaved and baked mica sheets, a series of specimens was obtained in a single vacuum cycle, providing information about the deposited films as a function of deposition time. Finally the vacuum was broken and the carbon backed specimens were floated off the mica carrier in HF-acid, rinsed in destilled water, caught on copper grids and inspected in a transmission electron microscope (Philips EM 200). Several photographs were taken from different parts of the specimen. The measurements were then carried out on these electron micrographs. For one set of deposition parameters R_1 (rate) and T (substrate temperature) twelve specimens with different deposition times were prepared.

3. Measurements

The evaluations of the micrographs were carried out with a Quantimet 720 image analysing computer. The principles of the measurements have been described previously [3, 4]. The following quantities were measured in all micrographs.

a) Number density of particles,
b) Area, covered with particles,
c) Projected vertical length of all particles,
d) Cluster diameter distributions (counting under conditions),
e) Distance distributions of clusters.

4. Theory

At very high supersaturations as present in deposition experiments in the UHV, the critical nucleus is very small and contains only a few atoms. In this case, the deposition process can be described by a simple atomic model, the kinetic nucleation theory [5]. In Fig. 1 the basic assumptions of this

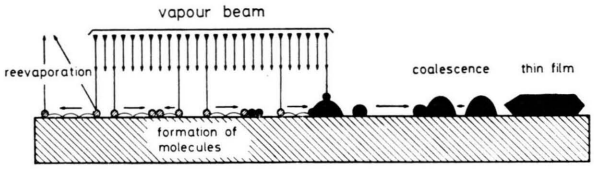

Fig. 1. Schematic presentation of processes ruling the heterogenous condensation: reevaporation, formation of molecules, coalescence and filling up stage.

model are presented. The deposited atoms, coming from the vapour source, have different destinations. A part of them is reflected immediately or delayed after a time of surface diffusion. Another part is trapped in defect sites or impacts with atoms under formation of biatomic molecules, others are forming triatomic molecules by impacts with diatomic molecules, and so on.

Greater aggregates are growing by atom addition from the adsorbed phase of single atoms or by direct impact with atoms from the vapour beam.

Greater crystallites have a certain mobility [6]. They are diffusing on the surface and coalesce with others under formation of crystal imperfections.

If there are point defects in the surface, a fractional part of the atoms is trapped in these defects. So the lifetime of a condensed atom is defined by reevaporation, trapping in defect sites and generation of biatomic molecules. Biatomic molecules are assumed to be the smallest stable nuclei in the absence of defect sites, while already single atoms can be stable nuclei in the case of appropriate defects.

In this case the well known rate equations [7] for the condensation process must be completed by a term for the defect site decoration.

$$\frac{dN_1}{dt} = R - \frac{N_1}{\tau_1} - K_1^+ N_1 L - 2 K_1 N_1^2 - N_1 \sum_{i=2}^{n_0} K_i N_i, \quad (1)$$

$$\frac{dN_2}{dt} = K_1 N_1^2 - K_2 N_1 N_2, \quad \text{etc.}$$

$$\tau_1 = \tau_0 \exp\{E_1/kT\}$$

is the residence time of the atoms at the surface.

$$K_1^+ = (a/\tau_0)(a + d_1) \exp\{-E_p/kT\}$$

is the collision factor for atomtrapping in adsorption sites, defined as product of the diffusion velocity of atoms and the cross section for this reaction.

τ_0 is the reciprocal Debye frequency, E_1 the adsorption energy and E_p the activation energy for surface diffusion. a is the lattice constant (or the jumping distance), d_1 the diameter of the adsorbed atoms and L the defect site concentration.

Using all these quantities it is possible to compute values from the experiments.

5. Experimental Results and Comparison with the Theory

5.1. Nucleation

Using the rate equations one obtains the nucleation rate, defined as the formation rate of stable aggregates. If defect sites are present, two contributions must be accounted for:

1. The formation rate of biatomic molecules in the case of statistical nucleation on a defect free surface and
2. the formation rate of atoms trapped in defect sites.

$$J = (dN/dt) = K_1^+ N_1 L + K_1 N_1^2. \quad (2)$$

At the very beginning of the condensation process, the reevaporation of atoms is predominant. Using the first differential equation of (1) we obtain $N_1 = R\tau_1$ and

$$J = K_1^+ R \tau_1 L + K_1 R^2 \tau_1^2. \quad (3)$$

For the comparison with the experiments, plots of the particle density versus deposition time for different deposition rates and substrate temperatures are needed. In Figs. 2 and 3 the particle density versus time is shown for a constant substrate temperature and different deposition rates and for a constant deposition rate and different substrate temperatures, respectively. The plots show the well known linear rise at small deposition times (slope = nucleation rate) and, after reaching a maximum density of particles caused by a balance of nucleation and coalescence, a decreasing particle number.

The slope of the curves and the height and position of the maxima depend strongly on the deposition rate and the substrate temperature. The theory

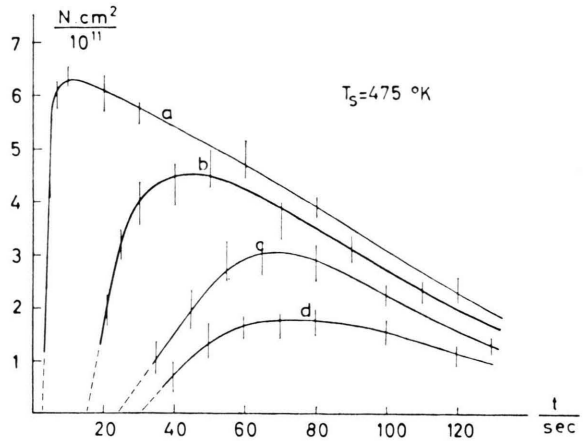

Fig. 2 Cluster density versus deposition time at $T_s = 475$ K.
a) $R = 2\,4 \cdot 10^{14}$ cm^{-2} s^{-1}; b) $R = 6.5 \cdot 10^{13}$ cm^{-2} s^{-1};
c) $R = 2.2 \cdot 10^{13}$ cm^{-2} s^{-1}; d) $R = 9.5 \cdot 10^{12}$ cm^{-2} s^{-1}.

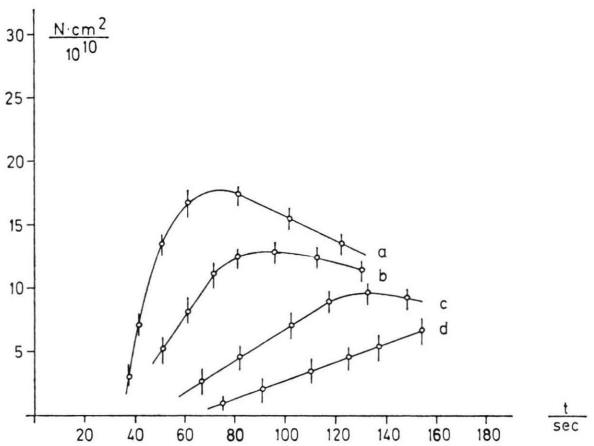

Fig. 3. Cluster density versus deposition time at $R = 9.5 \cdot 10^{12}$ cm^{-2} s^{-1}.
a) $T_s = 475$ K; b) $T_s = 575$ K; c) $T_s = 665$ K;
d) $T_s = 758$ K.

predicts a dependence of the nucleation rate on the deposition rate in that way that at low deposition rates a proportionality to R and at very high deposition rates a R^2 dependence should dominate. In Fig. 4 a qualitative agreement is visible. The slope of the curve starts at low deposition rates with the value 1 and tends toward the value 2 at the highest deposition rate, in contradiction to Poppa et al [8].

The dependence of the nucleation rate on the substrate temperature is obtained by rearranging Equation (3). For low deposition rates, neglecting

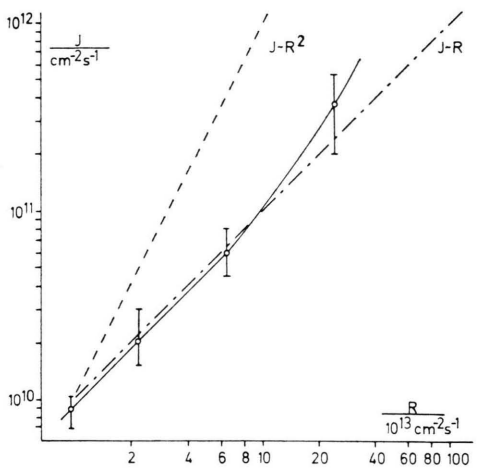

Fig. 4. Nucleation rate versus deposition rate at $T_s = 475$K.

the statistical nucleation

$$J \approx a(a + d_1) L R \exp\{(E_1 - E_p)/kT\} \qquad (4)$$

is obtained.

In Fig. 5 the nucleation rate is plotted against the reciprocal substrate temperature. Within the intervals of confidence a straight line with a slope related to $E_1 - E_p = 0.32$ eV is obtained.

An analysis of the preexponential allows an estimation of the defect site concentration. With plausible values for $a = d_1 = 3$ Å a value of $L \approx 5 \cdot 10^8$ cm^{-2} is obtained.

5.2 Growth of clusters

After nucleation the small particles are growing by addition of diffusing atoms. The growth rate is the product of the atom concentration and the collisionfactor

$$dN_i/dt = K_i N_1 .$$

In the micrographs only the measurement of diameters is possible but not that of volumes. With the assumption the crystallites to be hemispheres the time dependence of crystal growth is given by

$$d(t) = \left(\frac{2a}{\pi} V_1 R\right)^{1/2} t^{1/2} \exp\left[\frac{E_1 - E_p}{2kT}\right]. \qquad (5)$$

This equation describes the growth of individual crystals, only visible in in-situ experiments inside an UHV-electron microscope, as described by Poppa [9], Pócza [10] and Honjo [11]. The experiments in this paper only allow a comparison of the increase of the mean particle diameter with deposition time.

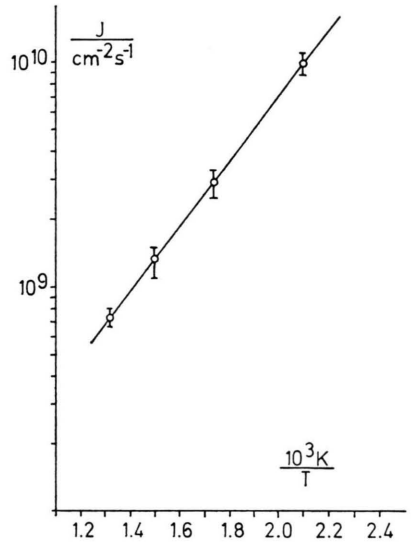

Fig. 5. Nucleation rate versus recipocal temperature at $R = 9.5 \cdot 10^{12}\ \mathrm{cm^{-2}\,s^{-1}}$.

In Fig. 6 the mean crystal diameter is plotted against the square root of time. Straight lines starting in the origin are obtained with a slope related to $E_1 - E_p = 0.34 \pm 0.04$ eV, in accordance with the result of the nucleation experiments.

5.3. Surface coverage

The surface area covered with crystallites is given by the product of the number density of crystallites and the mean projected area of the aggregates.

$$S = J t \frac{\pi}{4} \bar{d}^2 .$$

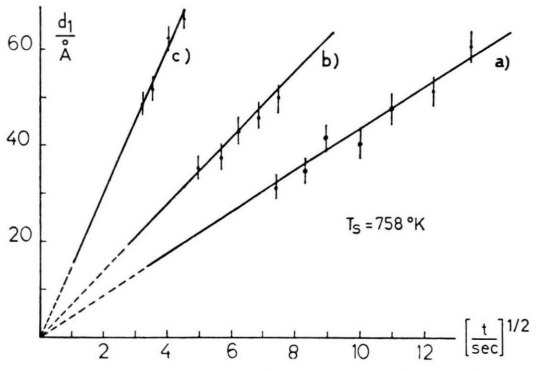

Fig. 6. Timedependence of the mean cluster diameter at $T = 758$ K.
a) $R = 9.5 \cdot 10^{12}\ \mathrm{cm^{-2}\,s^{-1}}$; b) $R = 2.2 \cdot 10^{13}\ \mathrm{cm^{-2}\,s^{-1}}$;
c) $R = 6.5 \cdot 10^{13}\ \mathrm{cm^{-2}\,s^{-1}}$.

Using Eqs. (3) and (5):

$$S(t) = \frac{a^2}{2}(a + d_1) L V_1 R^2 \exp\left[\frac{2E_1 - 2E_p}{kT}\right] t^2 + \frac{4a^2}{\pi} d_1 \tau_0 V_1 R^3 \exp\left[\frac{3E_1 - 2E_p}{kT}\right] t^2 . \quad (6)$$

The dependence of the nucleation rate on the deposition rate has shown that the nucleation at defect sites is predominant at least at low deposition rates. In this case the second term in (6) can be neglected. In Fig. 7 a plot of S versus t^2 is shown. The covered area increases with the square of the deposition time until a value is reached where large scale coalescence takes place. In this case a deviation of the predicted curve is visible. Using these curves, $2E_1 - 2E_p$ can be computed. One obtains $2E_1 - 2E_p = 0.74 \pm 0.08$ eV in good agreement with the energy parameters obtained before.

If we devide $S(t)$ by R^2, we obtain a constant value of $7 \cdot 1 \cdot 10^{29}\ \mathrm{cm^4\,s^2}$, independent of the deposition rate. In this case the value of L can be estimated with plausible values for $a = d_1 = 3$ Å. The defect site concentration is approximately $L = 3 \cdot 10^8\ \mathrm{cm^{-2}}$, in agreement with the value obtained by use of the nucleation rate.

Conclusions

The kinetic nucleation theory was shown to be applicable not only in the case of statistical heterogenous nucleation on substrates but also in the case of surfaces with point defects. The nucleation on

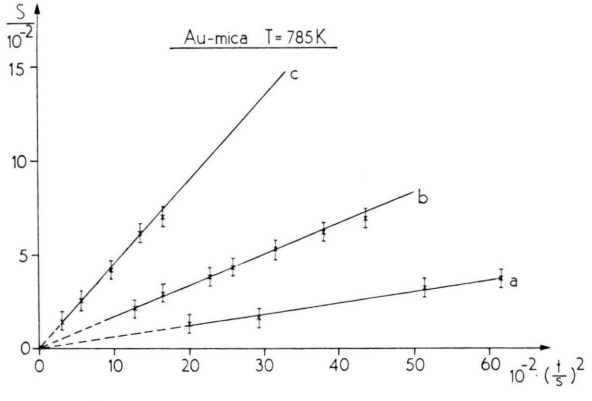

Fig. 7. Fractional part of the surface covered with clusters $T_s = 785$ K.
a) $R = 9.5 \cdot 10^{12}\ \mathrm{cm^{-2}\,s^{-1}}$; b) $R = 2.2 \cdot 10^{13}\ \mathrm{cm^{-2}\,s^{-1}}$;
c) $R = 6.5 \cdot 10^{13}\ \mathrm{cm^{-2}\,s^{-1}}$.

defect sites influences strongly the behaviour of the nucleation rate, especially concerning its dependence on the deposition rate and the substrate temperature. It is possible to obtain data for $E_1 - E_p$ and the defect site concentration.

The growth of clusters is not influenced by the defect concentration. The starting point of all computations is the fact that there are nuclei to be enlarged, independend of their origin. The quantity to be computed by use of the experimental data is the value of $E_1 - E_p$.

The surface coverage depends strongly on the mean particle diameter and the nucleation rate. So this quantity allows another estimation of $E_1 - E_2$.

Up to now it is not quite clear whether the identification of E_1 and E_p with the adsorption energy and the activation energy for surface diffusion is realistic or not. The accordance of the results for $E_1 - E_p$ using different experimental values shows only the consistency of the kinetic model.

Acknowledgement

We have to thank the "Deutsche Forschungsgemeinschaft" for enabling us to do this work by providing the Quantimet.

[1] H. Schmeißer, Vak. Techn. **21**, 165 (1972).
[2] H. Poppa and E. A. Lee, Thin Solid Films **32**, 223 (1976).
[3] C. F. Fisher, Microscope **19**, 1 (1971).
[4] H. Schmeißer and M. Harsdorff, Thin Solid Films **14**, 321 (1972)
[5] G. Zinsmeister, Vacuum **16**, 529 (1966)
[6] A. Masson, J. J. Metois, and R. Kern, J. Cryst. Growth **34**, 196 (1968).
[7] H. Schmeißer and M. Harsdorff, Z. Naturforsch. **25a**, 1896 (1970)
[8] E. H. Lee, H. Poppa, and G. M. Pound, Thin Solid Films **32**, 229 (1976).
[9] H. Poppa, J. Appl. Phys. **38**, 3883 (1967)
[10] J. F. Pócza, A. Barna, and P. B. Barna, J. Vac. Sci. & Techn. **6**, 427 (1969).
[11] K. Yagi, K. Takayanagi, K. Kobayashi, and G. Honjo, Thin Solid Films **32**, 185 (1976).